INSTITUTE OF PHYSICS PUBLISHING JOURNAL OF OPTICS B: QUANTUM AND SEMICLASSICAL OPTICS

J. Opt. B: Quantum Semiclass. Opt. **5** (2003) S119–S123 PII: S1464-4266(03)57336-0

Bose–Einstein condensation in a magnetic double-well potential

T G Tiecke, M Kemmann, Ch Buggle, I Shvarchuck, W von Klitzing and J T M Walraven

FOM Institute for Atomic and Molecular Physics, Kruislaan 407, 1098 SJ Amsterdam, The Netherlands

Received 29 November 2002, in final form 13 January 2003
Published 2 April 2003
Online at stacks.iop.org/JOptB/5/S119

Abstract

We present the first experimental realization of Bose–Einstein condensation in a purely magnetic double-well potential. This has been achieved by combining a static Ioffe–Pritchard trap with a time orbiting potential. The double trap can be rapidly switched to a single-harmonic trap of identical oscillation frequencies, thus accelerating the two condensates towards each other. Furthermore, we show that time-averaged potentials can be used as a means to control the radial confinement of the atoms. Manipulation of the radial confinement allows vortices and radial quadrupole oscillations to be excited.

Keywords: Magnetic trapping, BEC, TOP, double TOP, TAP

1. Introduction

Bose–Einstein condensates (BEC) in dilute vapours have been studied using magnetic [1–3] and optical [4, 5] potentials. Magnetic traps can be divided into two classes: static and dynamic traps. Bose–Einstein condensation was first observed in a dynamic trap using a time orbiting potential (TOP) [1] and shortly thereafter in a static Ioffe–Pritchard trap [6]. A TOP trap uses a three-dimensional quadrupole field to confine the atoms. In order to avoid Majorana losses near the centre of the trap, a rotating homogeneous field shifts the field minimum onto a circle around the trapped sample. At an appropriate rotation frequency the trapping potential is simply the time average of the orbiting potential. The Ioffe–Pritchard trap on the other hand is designed to have a static, non-zero field minimum. In radial (x, y) directions the atoms are confined by a quadrupole field. On the z-axis the radial field component is zero and the axial component is a parabola, $B_z = B_0 + \frac{1}{2}\beta z^2$, with a curvature β and an offset B_0.

In this paper we explore the possibilities offered by time-averaged potentials (TAP) in Ioffe–Pritchard traps. We distinguish two cases, $B_0 > 0$ and $B_0 < 0$. In the first case B_z is always positive and the axial confining potential is a parabola. We can influence the radial and axial confinement of the atoms by applying a *linear* TAP field, i.e. a homogeneous modulation field orthogonal to the z-axis. This allows us to introduce a radial ellipticity in the otherwise axially symmetric trap, which can be exploited to drive vortices or quadrupole oscillations. In the second case ($B_0 < 0$), B_z crosses zero at two points on the z-axis creating an axial double-well potential. We can make a double-TOP trap by adding a *circular* TAP field orthogonally to the z-axis [1, 7]. As an example, we demonstrate Bose–Einstein condensation in a double-TOP trap (see figure 1).

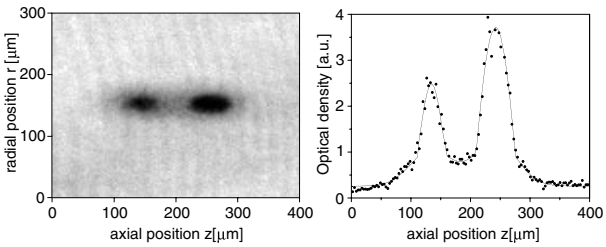

Figure 1. An absorption image of two BECs created in a double-TOP trap. The condensates have been accelerated towards each other by switching to a single trap. The picture was taken after 3 ms of free expansion. The figure on the right is an optical density profile through the centre of both condensates. The solid curve is a fit to the experimental data.

2. Trap geometry

We explored the possibilities offered by TAP fields in a Ioffe–Pritchard coil configuration using an efficient semi-analytic model of the trap. We calculate the magnetic field for

the detailed geometry of each coil separately over a three-dimensional grid around the trap centre. Two different regions are chosen: one for the cold atom cloud and the Bose–Einstein condensate ($10 \times 10 \times 100\ \mu\text{m}^3$) and one for the hot thermal cloud ($1 \times 1 \times 10\ \text{mm}^3$). On this grid a three-dimensional fourth-order polynomial is fitted for each of the coils. The final field is calculated as the sum over the polynomials with the electrical currents of the individual coils as parameters. The frequencies and non-linearities of the trap are then simply the appropriate coefficients of the final polynomial. Using these polynomials *any* field possible with our coil configuration can be rapidly calculated. For selected cases we also derive simplified analytical expressions to emphasize the principles involved.

In order to elucidate the TAP principle we write the potential $U(x, y, z)$ of the axially symmetric ($\omega_\rho \equiv \omega_x = \omega_y$) Ioffe–Pritchard trap in the approximation of a elongated trapping potential ($\omega_\rho \gg \omega_z$):

$$U(x, y, z) = \mu\sqrt{\alpha^2(x^2 + y^2) + \left(B_0 + \tfrac{1}{2}\beta z^2\right)^2} \qquad (1)$$

where α is the radial gradient, μ the magnitude of the magnetic moment of the atoms and m the atomic mass [8, 9]. For the standard Ioffe–Pritchard trap ($B_0 > 0$) the harmonic frequencies are

$$\omega_\rho = \sqrt{\frac{\mu}{m}\frac{\alpha^2}{B_0}}, \qquad \omega_z = \sqrt{\frac{\mu}{m}\beta}. \qquad (2)$$

2.1. Magnetic double-well potential ($B_0 \leqslant 0$)

For a negative offset the modulus of the field becomes zero at two points on the z-axis creating two three-dimensional quadrupole traps. The distance Δz between the two trap centres can be controlled via B_0:

$$\Delta z = 2\sqrt{2|B_0|/\beta}. \qquad (3)$$

Inversely, we can conveniently determine B_0 from a measurement of Δz.

To eliminate depolarization near the trap minima we use a circular TAP, creating a double-TOP configuration [7, 10]. A homogeneous field of amplitude B_m orthogonal to the z-axis displaces the magnetic field zero by a distance

$$\rho_m = B_m/\alpha. \qquad (4)$$

This expression is conveniently used to calibrate B_m.

Rotating the modulation field around the z-axis (with an angular modulation frequency ω_m) moves the zero along a so-called 'circle of death'. If the modulation frequency is large compared to the oscillation frequency of the atoms in the time-averaged trap but slow compared to the Larmor frequency ($\overline{\omega}_{\rho,z} \ll \omega_m \ll \mu B_m/\hbar$), the atoms will see the time average of the modulated potential [10]:

$$U_{\text{TAP}}(x, y, z) = \frac{1}{2\pi}\int_0^{2\pi} U(x + \rho_m \sin\phi, y + \rho_m \cos\phi, z)\,\mathrm{d}\phi. \qquad (5)$$

The harmonic trapping frequencies for both minima of the double-well potential are

$$\overline{\omega}_\rho = \sqrt{\frac{\mu}{m}\frac{\alpha^2}{2B_m}}, \qquad \overline{\omega}_z = \sqrt{\frac{\mu}{m}\frac{2\beta|B_0|}{B_m}}. \qquad (6)$$

Note that $\overline{\omega}_z = 0$ for $B_0 = 0$ and $B_m > 0$. For this case the axial confinement is governed purely by higher-order terms.

The two traps are separated by a potential barrier of

$$U_{\text{barrier}} = \mu\left(\sqrt{B_0^2 + B_m^2} - B_m\right) \qquad (7)$$

where the first term in the brackets corresponds to the field at the origin and B_m to the field minimum of each of the wells.

One of the interesting aspects of this double trap is the possibility of rapidly switching from the double-TOP trap to a static Ioffe–Pritchard trap. This is done by removing the TAP field and switching from $B_0 < 0$ to $B_0' > 0$, changing neither α nor β. The condensates then accelerate towards each other and collide in the origin at a *relative* kinetic energy of $E_{\text{kin}} = 2\mu|B_0|$. In a harmonic trap the shape of a cloud is completely decoupled from its centre-of-mass motion. Therefore, if the trapping frequencies in the single and double traps are equal, the gas clouds move towards each other without changing shape. It follows from equations (2) and (6) that the axial *and* radial frequencies of the double and single traps are the same if the offset and modulation fields obey

$$B_0' = 2B_m = -4B_0. \qquad (8)$$

In our trap we can easily explore collision energies up to 1.3 mK corresponding to 7000 recoil energies at 780 nm.

Let us turn to the question of gravity. If the trap is slightly tilted, gravity will affect the relative depth of the two potential minima and thus the relative number of atoms in the two traps. As the distance between the traps increases the difference in atom numbers continues to grow. If the traps were to remain coupled all atoms would eventually collect in the lower trap. Therefore the two traps have to be separated sufficiently quickly.

2.2. Magnetic single-well potential ($B_0 > 0$)

For a positive offset we have a standard Ioffe–Pritchard potential and we distinguish two types of TAP: the linear and circular TAPs.

2.2.1. Linear TAP and radial ellipticity. If we apply a linear TAP field in the x-direction modulating at an angular frequency ω_m we can write the TAP as

$$U_{\text{TAP}}(x, y, z) = \frac{1}{2\pi}\int_0^{2\pi} U(x + \rho_m \sin\phi, y, z)\,\mathrm{d}\phi. \qquad (9)$$

The radial harmonic trap frequencies ($\overline{\omega}_x, \overline{\omega}_y$) can be expressed in terms of the ratio $b \equiv B_m/B_0$:

$$\overline{\omega}_x = \omega_\rho\sqrt{\frac{\mathsf{E}'(b)}{1 + b^2}}, \qquad \overline{\omega}_y = \omega_\rho\sqrt{\mathsf{K}'(b)}, \qquad (10)$$

where[1] $\mathsf{K}'(b) = \frac{1}{2\pi}\int_0^{2\pi}(1 + b^2\sin^2\phi)^{-1/2}\,\mathrm{d}\phi$ and $\mathsf{E}'(b) = \frac{1}{2\pi}\int_0^{2\pi}(1 + b^2\sin^2\phi)^{1/2}\,\mathrm{d}\phi$. The axial frequency becomes

$$\overline{\omega}_z = \omega_z\sqrt{\mathsf{K}'(b)}. \qquad (11)$$

[1] Note that the integrals E' and K' used in equations (10) and (11) are related to the elliptical integrals E and K as $\mathsf{E}'(b) = 2\mathsf{E}(-b^2)/\pi$ and $\mathsf{K}'(b) = 2\mathsf{K}(-b^2)/\pi$.

For $b \ll 1$ the ellipticity is given by

$$\epsilon \equiv \frac{\overline{\omega}_x^2 - \overline{\omega}_y^2}{\overline{\omega}_x^2 + \overline{\omega}_y^2} \approx -b^2/4. \tag{12}$$

For $b = 1$, using equations (10) we calculate $\epsilon = -0.16$.

Radial ellipticity can be used for example to excite quadrupole oscillations or to create vortices in a BEC [11]. To drive the radial quadrupole oscillation, the ellipticity of the trap has to be modulated for example by driving the fields as $B_x(t) = B_m \sin(\omega_m t)(1 + \sin \Omega t)/2$ and $B_y(t) = B_m \cos(\omega_m t)(1 - \sin \Omega t)/2$, where Ω is matched to the frequency of the quadrupole oscillation.

Vortices can be created by rotating an elliptic trapping potential at an angular frequency Ω. This has been demonstrated using rotating laser beams in a magnetic trap [12, 13] and in an asymmetric TOP trap [14, 15]. We can do this by rotating the linear TAP field as $B_x(t) = B_m \sin \omega_m t \sin \Omega t$ and $B_y(t) = B_m \sin \omega_m t \cos \Omega t$.

2.2.2. Circular TAP and shape oscillations of a Bose–Einstein condensate. Applying a circular TAP results in the trapping potentials

$$U_{\mathrm{TAP}}(x, y, z) = \frac{1}{2\pi} \int_0^{2\pi} U(x + \rho_m \sin \phi, y + \rho_m \cos \phi, z)\, \mathrm{d}\phi. \tag{13}$$

The radial and axial harmonic trap frequencies $(\overline{\omega}_\rho, \overline{\omega}_z)$ are then

$$\overline{\omega}_\rho = \omega_\rho \frac{(1 + \frac{1}{2}b^2)^{1/2}}{(1 + b^2)^{3/4}}, \qquad \overline{\omega}_z = \omega_z (1 + b^2)^{-1/4}, \tag{14}$$

where ω_ρ and ω_z are given in equation (2). We can now control the axial and radial trapping frequencies using only the relatively small offset and modulation fields. The modulation b lowers the axial and radial frequencies whereas the offset B_0 affects the radial confinement only. This can be used to excite shape oscillations.

An axially symmetric shape oscillation of small amplitude at a frequency ω_s is described by

$$\rho_{\mathrm{TF}}(t) = \rho_{\mathrm{TF}}(1 + a_\rho \cos(\omega_s t)), \qquad z_{\mathrm{TF}}(t) = z_{\mathrm{TF}}(1 + a_z \cos(\omega_s t)), \tag{15}$$

where ρ_{TF} and z_{TF} are the radial and axial Thomas–Fermi sizes. The two lowest-order axially symmetric modes of a condensate [16–18] have frequencies of $\omega_{\mathrm{Q}} = \sqrt{5/2}\,\omega_z$ and $\omega_{\mathrm{B}} \simeq 2\omega_\rho$ and oscillate with

$$a_\rho/a_z = -1/4 \qquad \text{and} \qquad a_\rho/a_z = \omega_\rho/\omega_z \tag{16}$$

respectively. We can start a *pure* shape oscillation by creating a steady-state condensate in one trap and suddenly switching to a different trap. The steady-state condensate has to fulfil the conditions for $\rho_{\mathrm{TF}}(0)$ and $z_{\mathrm{TF}}(0)$ of equations (15), where the amplitudes a_ρ and a_z have to be chosen according to one of the equations (16) depending on the choice of mode. The steady-state Thomas–Fermi sizes in the second trap are ρ_{TF} and z_{TF}.

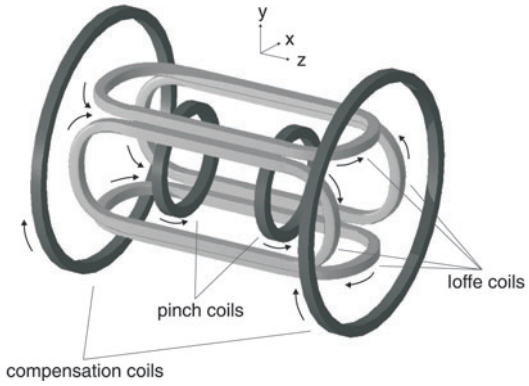

Figure 2. The coil configuration of our Ioffe–Pritchard trap. The arrows indicate the directions of the currents in the main coils. Modulation coils (not shown) are attached to the outside faces of the Ioffe coils.

Since the atom numbers in the two harmonic traps are the same, it can be shown that the frequencies in the traps and the corresponding Thomas–Fermi sizes are related as

$$\frac{\omega'_\rho}{\omega_\rho} = \left(\frac{z_{\mathrm{TF}}}{z'_{\mathrm{TF}}}\right)^{1/2} \left(\frac{\rho_{\mathrm{TF}}}{\rho'_{\mathrm{TF}}}\right)^2, \qquad \frac{\omega'_z}{\omega_z} = \left(\frac{z_{\mathrm{TF}}}{z'_{\mathrm{TF}}}\right)^{3/2} \left(\frac{\rho_{\mathrm{TF}}}{\rho'_{\mathrm{TF}}}\right). \tag{17}$$

Let us now look at the case where we excite a shape oscillation by switching between a TAP trap to a standard Ioffe–Pritchard trap. For a small amplitude ($a_\rho, a_z \ll 1$), we calculate B_0 for a given modulation ratio b:

$$\frac{B_0}{B'_0} = \frac{1 + \frac{1}{2}b^2}{(1 + b^2)^{\frac{3}{2}}} \left\{1 - \frac{1 + 4\frac{a_\rho}{a_z}}{3 + 2\frac{a_\rho}{a_z}} [1 - (1 + b^2)^{-\frac{1}{4}}]\right\}^{-2}, \tag{18}$$

where, as before, B'_0 is the offset in the non-modulated trap. This equation simplifies for the lower-lying mode ($a_\rho/a_z = -1/4$) to

$$\frac{B_0}{B'_0} = \frac{1 + \frac{1}{2}b^2}{(1 + b^2)^{\frac{3}{2}}}. \tag{19}$$

In this mode we can excite a 10% oscillation ($a_z = 0.1$) starting from a normal Ioffe–Pritchard trap by adiabatically ramping the modulation from zero to $b = 0.78$ and at the same time lowering the offset to 64% of its original value ($B_0 = 0.64 B'_0$). Reverting quickly to the original parameters then starts an oscillation of the condensate in the *pure* lower-lying axially symmetric mode without the need to alter the large currents in the Ioffe and compensation coils.

3. BEC in a double TOP

As an example of the use of TAP in combination with a Ioffe–Pritchard coil configuration, we demonstrate Bose–Einstein condensation in a double-TOP trap.

Our Ioffe–Pritchard trap is shown in figure 2 and is described in detail in [19]. The trap consists of four Ioffe coils producing the radial quadrupole field. The field of the pinch coils provides the axial parabolic potential. The compensation

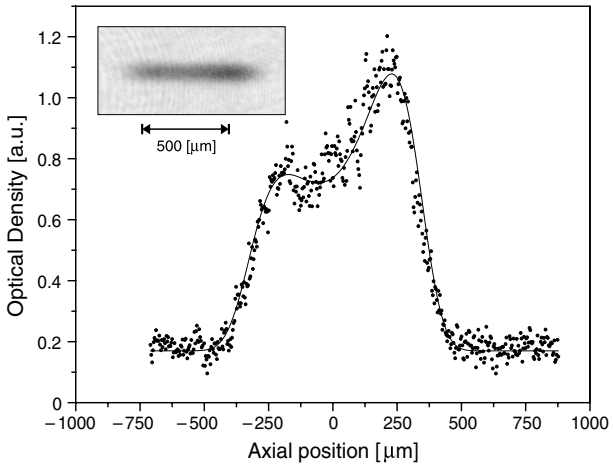

Figure 3. An optical density profile along the z-axis of the thermal cloud during the early stages of separation after a free expansion of 4 ms. The cloud contains 10^6 atoms at a temperature of 0.66 μK as determined from the radial expansion. The solid curve is a prediction from the model with the angle (0.4°) and maximal optical density as adjustable parameters. The inset shows the absorption image.

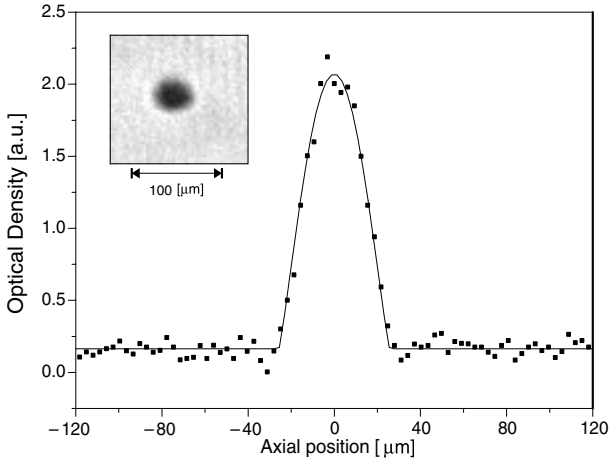

Figure 4. An optical density profile along the z-axis of one of the two BECs after 4 ms of free expansion. The solid curve is a fit of a Thomas–Fermi profile to the experimental points. The BEC contains 4×10^4 atoms. The inset shows the absorption image.

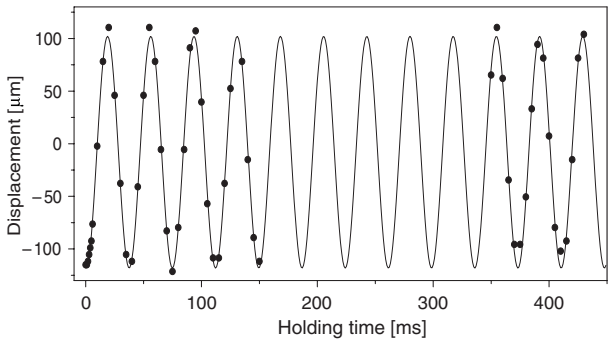

Figure 5. An axial centre-of-mass oscillation of a Bose–Einstein condensate in a double-well trap. The solid curve corresponds to a fit of a sine function to the data ($\omega_z = 2\pi \times 26.8$ Hz).

coils are designed to compensate the field of the pinch coils at the origin. The two sets of coils are connected in series in order to reduce field noise. The offset B_0 is controlled by applying a dedicated homogeneous field (coils not shown in figure 2). In order to be able to create the modulation fields, we have attached modulation coils to the outer faces of the Ioffe coils. They consist of PCB boards with one 35 μm layer of copper on either side, connected in series. In order to maximize the trap stability, facing modulation coils were driven in series.

The experimental path towards the BEC into the magnetic double well is as follows. We optically pump about 6×10^9 atoms from a ^{87}Rb MOT into the $|5^2S_{1/2}, F = 2, m_F = 2\rangle$ state. These are loaded into a matching, horizontal Ioffe–Pritchard trap ($\omega_\rho = 2\pi \times 8$ Hz, $\omega_z = 2\pi \times 7$ Hz and $B_0 = 37$ G). The circular TAP field of $B_m = 0.68(3)$ G rotating at a frequency of 7.0 kHz remains constant throughout the experiment[2]. The transfer efficiency is about 50% and the temperature in the trap is about 70 μK. We then compress the trap to $\omega_\rho = 2\pi \times 390(10)$ Hz and $\omega_z = 2\pi \times 14.8(4)$ Hz by ramping the currents in the main coils from 50 A up to their final value of 400 A and reducing the offset to $B_0 = 0.4$ G. At this current we have[3] $\alpha = 352(1)$ G cm^{-1} and $\beta = 266(2)$ G cm^{-2} [20].

Rapid forced evaporation using a radio-frequency sweep-down to an intermediate value of 433 kHz above the bottom of the trap cools the sample to a temperature of about 8 μK. At this temperature, 90% of the atoms lie within the future circle of death. We then ramp the offset field B_0 linearly down at a rate of -0.5 G s^{-1}, eventually splitting the cloud.

Figure 3 shows a profile through a thermal cloud of 10^6 atoms at a temperature of 0.66 μK during the early stages of the splitting process at $B_0 = -53(1)$ mG. The temperature and atom number were determined by time-of-flight imaging. The solid curve is calculated for the measured temperature using the semi-analytical model adjusting the maximum optical density and the tilt angle (0.4°) to fit the data.

After the cloud is fully split we fix the offset at $B_0 = -0.63(1)$ G and condense the sample by lowering the radio-frequency to 23 kHz above the bottom of the trap. Figure 4 shows a profile of an absorption image of one of the two BECs after a free expansion of 4 ms. The solid curve is a fit to the Thomas–Fermi distribution in a harmonic trap. The condensate contains 4×10^4 atoms.

We excited a centre-of-mass oscillation of a BEC along the z-axis by jumping the offset B_0 from $-0.43(1)$ to $-0.63(1)$ G thus shifting the traps by 115(1) μm outwards. The condensates started to oscillate around the new trap centre (dots in figure 5). The solid curve is a fit of a sine wave to the data ($\omega_z = 2\pi \times 26.8$ Hz). From our semi-analytical model including an anharmonic shift of 0.8 Hz, we find a frequency of 27.5(8) Hz. Hence we have agreement with the data within the experimental error.

4. Conclusions and outlook

We explored the TAP principle as a powerful tool for manipulating Ioffe–Pritchard traps. For a positive B_0, the radial confinement can be influenced using small modulation fields, e.g. to excite vortices and pure shape oscillations. For

[2] The modulation current of $I \approx 3$ A corresponding to the modulation field of $B_m = 0.68(3)$ G was driven by a standard audio-amplifier (Yamaha AX-496).

[3] α and β have been determined from B_0 and the oscillation frequencies.

a negative B_0, double-well potentials are obtained. These can readily be converted to a single trap and thus used in collision experiments with ultracold gas clouds. As an example we used a circular TAP field to demonstrate Bose–Einstein condensation in a double-TOP trap.

Acknowledgments

We would like to thank Dima Petrov for critical remarks. This work is part of the research programme of the Stichting voor Fundamenteel Onderzoek der Materie (FOM) which is financially supported by the Nederlandse Organisatie voor Wetenschappelijk Onderzoek (NWO).

References

[1] Anderson M H, Ensher J R, Matthews M R, Wieman C E and Cornell E A 1995 Observation of Bose–Einstein condensation in a dilute atomic vapor *Science* **269** 198–201

[2] Bradley C C, Sackett C A, Tollett J J and Hulet R G 1995 Evidence of Bose–Einstein condensation in an atomic gas with attractive interactions *Phys. Rev. Lett.* **75** 1687–90

[3] Davis B, Mewes M O, Andrews M R, Vandruten N J, Durfee D S, Kurn D M and Ketterle W 1995 Bose–Einstein condensation in a gas of sodium atoms *Phys. Rev. Lett.* **75** 3969–73

[4] Barrett M D, Sauer J A and Chapman M S 2001 All-optical formation of an atomic Bose–Einstein condensate *Phys. Rev. Lett.* **87** 010404

[5] Stamper-Kurn D M, Andrews M R, Chikkatur A P, Inouye S, Miesner H-J, Stenger J and Ketterle W 1998 Optical confinement of a Bose–Einstein condensate *Phys. Rev. Lett.* **80** 2027–30

[6] Mewes M-O, Andrews M R, Vandruten N J, Kurn D M, Durfee D S and Ketterle W 1996 Bose–Einstein condensation in a tightly confining dc magnetic trap *Phys. Rev. Lett.* **77** 416–19

[7] Thomas N R, Wilson A C and Foot C J 2002 Double-well magnetic trap for Bose–Einstein condensates *Phys. Rev.* A **65** 063406

[8] Bergeman T, Erez G and Metcalf H 1987 Magnetostatic trapping fields for neutral atoms *Phys. Rev.* A **35** 1535–46

[9] Surkov E L, Walraven J T M and Shlyapnikov G V 1994 Collisionless motion of neutral particles in magnetostatic traps *Phys. Rev.* A **49** 4778–86

[10] Petrich W, Anderson M H, Ensher J R and Cornell E A 1995 Stable, tightly confining magnetic trap for evaporative cooling of neutral atoms *Phys. Rev. Lett.* **74** 3352–5

[11] Walsworth R and You L 1997 Selective creation of quasiparticles in trapped Bose condensates *Phys. Rev.* A **56** 555–9

[12] Madison K W, Chevy F, Wohlleben W and Dalibard J 2000 Vortex formation in a stirred Bose–Einstein condensate *Phys. Rev. Lett.* **84** 806–9

[13] Abo-Shaeer J R, Raman C, Vogels J M and Ketterle W 2001 Observation of vortex lattices in Bose–Einstein condensates *Science* **292** 476–9

[14] Hodby E, Hechenblaikner G, Hopkins S A, Maragò O M and Foot C J 2002 Vortex nucleation in Bose–Einstein condensates in an oblate, purely magnetic potential *Phys. Rev. Lett.* **88** 010405

[15] Haljan P C, Coddington I, Engels P and Cornell E A 2001 Driving Bose–Einstein-condensate vorticity with a rotating normal cloud *Phys. Rev. Lett.* **87** 210403

[16] Stringari S 1996 Collective excitations of a trapped Bose-condensed gas *Phys. Rev. Lett.* **77** 2360–3

[17] Fort C, Prevedelli M, Minardi F, Cataliotti F S, Ricci L, Tino G M and Inguscio M 2000 Collective excitations of a Rb-87 Bose condensate in the Thomas–Fermi regime *Europhys. Lett.* **49** 8–13

[18] Chevy F, Bretin V, Rosenbusch P, Madison K W and Dalibard J 2002 Transverse breathing mode of an elongated Bose–Einstein condensate *Phys. Rev. Lett.* **88** 250402

[19] Dieckmann K 2001 Bose–Einstein condensation with high atom number in a deep magnetic trap *PhD Thesis* University of Amsterdam
www.amolf.nl/publications/theses/dieckmann

[20] Shvarchuck I, Buggle Ch, Petrov D S, Dieckmann K, Zielonkowski M, Kemmann M, Tiecke T G, von Klitzing W, Shlyapnikov G V and Walraven J T M 2002 Bose–Einstein condensation into non-equilibrium states studied by condensate focusing *Phys. Rev. Lett.* **89** 270404 (*Preprint* cond-mat/0207599)